International Journal of Mechanical, Industrial and Aerospace Sciences
ISSN: 2517-9950
Vol:13, No:2, 2019

Multi-Temporal Urban Land Cover Mapping Using Spectral Indices

Mst Ilme Faridatul, Bo Wu

***Abstract*—**Multi-temporal urban land cover mapping is of paramount importance for monitoring urban sprawl and managing the ecological environment. For diversified urban activities, it is challenging to map land covers in a complex urban environment. Spectral indices have proved to be effective for mapping urban land covers. To improve multi-temporal urban land cover classification and mapping, we evaluate the performance of three spectral indices, e.g. modified normalized difference bare-land index (MNDBI), tasseled cap water and vegetation index (TCWVI) and shadow index (ShDI). The MNDBI is developed to evaluate its performance of enhancing urban impervious areas by separating bare lands. A tasseled cap index, TCWVI is developed to evaluate its competence to detect vegetation and water simultaneously. The ShDI is developed to maximize the spectral difference between shadows of skyscrapers and water and enhance water detection. First, this paper presents a comparative analysis of three spectral indices using Landsat Enhanced Thematic Mapper (ETM), Thematic Mapper (TM) and Operational Land Imager (OLI) data. Second, optimized thresholds of the spectral indices are imputed to classify land covers, and finally, their performance of enhancing multi-temporal urban land cover mapping is assessed. The results indicate that the spectral indices are competent to enhance multi-temporal urban land cover mapping and achieves an overall classification accuracy of 93-96%.

***Keywords*—**Land cover, mapping, multi-temporal, spectral indices

I. Introduction

URBAN land cover analysis is important to study the geographic environment [1]. The changes in urban land covers affect the ecological environment [2]. Up-to-date information on land covers and multi-temporal mapping is of paramount importance for monitoring the changes in the urban ecosystem, and is also important for managing urban sprawl, and regional and local level planning [3]. It is highly desirable to develop reliable methods of mapping urban land covers. The urban diversified activities, and spatial and temporal variations imply a challenge to classifying and mapping land covers in these areas [4]. Over the past decades, remote sensing data have proved efficient for mapping land covers and monitoring multi-temporal changes [5]. Various land cover classification approaches have been used to map land covers [3], [6]-[9]. However, it is difficult to select the best classifiers because each of the methods has its own strengths and limitations.

Mapping of land covers using spectral indices has proved to be effective. Because the spectral index values primarily characterize a particular land cover [10] and demonstrate the relative abundance of features of interest [11].

Over the past decades, various spectral indices have been developed and used for detecting different geographic features. Zha et al. [12] developed the normalized difference built-up index (NDBI) to map urban built-up areas. McFeeters [13] developed the normalized difference water index (NDWI) to delineate open water features. Xu [14] enhanced water detection by developing the MNDWI. Rouse et al. [15] developed the normalized difference vegetation index (NDVI) for extracting vegetation. The tasseled cap (TC) indices have been used for extracting information on soil, water, and vegetation [16]. In addition to the individual indices, various combination of spectral indices has been used for mapping urban land covers based on automatic and semi-automatic classifiers. For example, Li et al. [3] classified urban land covers based on the NDVI, vegetation and water masking index (VWMI), bright impervious surface binary (BISB), and normalized difference bare land index (NDBLI). A semiautomatic segmentation approach was implemented by He et al. [7] to map urban built-up areas. Bhatt et al. [17] applied object-based classification using the NDVI, MNDWI, and modified soil adjusted vegetation index (SAVI).

Although various classification approaches are available, precise land cover mapping in a heterogeneous urban environment is still a challenge and it is an ongoing subject of research. For enhancing urban land cover classification, Faridatul and Wu [10] develop three novel spectral indices, the MNDWI, TCWVI, and ShDI. However, the previous study used only Landsat-8 OLI data for evaluating the performance of the spectral indices and urged to evaluate their performance to other sensors. In this backdrop, this paper aims to evaluate the performance of the spectral indices for multi-temporal urban land cover mapping using data from multiple sensors e.g., Landsat ETM, TM, and OLI. Following the introduction, Section II describes the study area and datasets, and illustrates the approach of classifying multi-temporal land covers using spectral indices. Section III presents in detail the experimental evaluation and results. Finally, Section IV draws the conclusions and discussion.

II. Data and Methods

A. Study Area and Datasets

Hong Kong, the special administrative region of China, is

M. I. Faridatul is with the Department of Land Surveying and Geo-Informatics, The Hong Kong Polytechnic University, Hong Kong, and also with the Department of Urban and Regional Planning, Rajshahi University of Engineering & Technology, Bangladesh (e-mail: ilme.faridatul@connect.polyu.hk).

B. Wu is with the Department of Land Surveying and Geo-Informatics, The Hong Kong Polytechnic University, Hong Kong (corresponding author, phone: +852 2766 4335, e-mail: bo.wu@polyu.edu.hk).

selected as the study area. It is situated between latitudes 22°09' to 23°37' and longitudes 113°52' to 114°30'. The entire area of Hong Kong is 1,095 km^2; to evaluate the proposed approach an area of 256 km^2 is selected. This study uses representative data from three sensors: Landsat-7 ETM, Landsat-5 TM and Landsat-8 OLI for evaluation and comparison analysis. Landsat images are obtained from the US Geological Survey EarthExplorer (https://earthexplorer.usgs.gov). The map projection of the collected images is the Universal Transverse Mercator (UTM) within Zone 49N Datum World Geodetic System (WGS) 84. For validating, we have tried to collect similar dated high-resolution images for each study year but due to data scarcity, only high-resolution multispectral image ZY-3 collected in 2013 is used for validation. Table I lists the multi-temporal datasets of Hong Kong.

B. Overview of Approach

This paper presents the performance of three spectral indices for multi-temporal land cover mapping using data from multiple sensors. In this research, urban land covers are classified into four major categories e.g., water, vegetation, bare land, and impervious areas (Table II). Because these land covers are the fundamental components of an urban environment [3], [18]. In the first stage, the suitability of the spectral indices derived from multiple sensors is evaluated by comparative analysis. In the second stage, land cover classifications derived from the spectral indices are used for evaluating their performance for multi-temporal urban land cover mapping.

TABLE I
MULTI-TEMPORAL DATA

Sensor	Date	Resolution (m/pixel)
Landsat-7 ETM	2000-11-01	30
Landsat-5 TM	2010-12-23	30
Landsat-8 OLI	2013-12-31	30
ZY-3	2013-03-08	5.8

TABLE II
DESCRIPTION OF THE LAND COVER CLASSES

Classes	Descriptions	Abbreviation
Impervious areas	Commercial, industrial, residential, transport, and any other built structures	IA
Surface water	Ponds, rivers, canals, low-lying areas with seasonal water, and any other open bodies of water	SW
Vegetation	Forests, trees, gardens, and any other vegetated surfaces	V
Bare lands	Sparse grassland, open spaces, and any other non-impervious areas	BL

In this research, first, Landsat level 1 data are collected and applied atmospheric correction. Second, the indices are developed using atmospherically corrected spectral bands. The MNDBI is developed using the spectral bands shortwave infrared 2 and blue as (1). The combination of these two bands results in positive values for bare land only, and negative values for all of the other land cover types. The TCWVI is developed using the tasseled cap brightness index (TC_{BI}) and the tasseled cap greenness index (TC_{GI}). The use of TC_{BI} and TC_{GI} as (2) yields the highest positive values for water and the lowest values for vegetation thus facilitates the simultaneous detection of water and vegetation. The ShDI is developed as (3) to enhance water detection by separating building shadows.

$$\mathrm{MNDBI} = \frac{(\rho_{\mathrm{SWIR2}} - \rho_{\mathrm{Blue}})}{(\rho_{\mathrm{SWIR2}} + \rho_{\mathrm{Blue}})} \quad (1)$$

where ρ_{SWIR2} and ρ_{Blue} represent reflectance values of the shortwave infrared 2 and blue bands.

$$\mathrm{TCWVI} = \frac{(\mathrm{TC_{BI}} - \mathrm{TC_{GI}})}{(\mathrm{TC_{BI}} + \mathrm{TC_{GI}})} \quad (2)$$

where TC_{BI} and TC_{GI} represent TC_{BI} and TC_{GI}, respectively.

$$\mathit{Sh}\mathrm{DI} = \left[\frac{2 * \rho_{\mathrm{NIR}} - \rho_{\mathrm{SWIR2}}}{2 * \rho_{\mathrm{NIR}} + \rho_{\mathrm{SWIR2}}}\right] - \left[\frac{\rho_{\mathrm{NIR}} - \rho_{\mathrm{Blue}}}{\rho_{\mathrm{NIR}} + \rho_{\mathrm{Blue}}}\right] + 4 * \rho_{\mathrm{Red}} \quad (3)$$

where ρ_{NIR}, ρ_{SWIR2}, ρ_{Blue}, and ρ_{Red} represent reflectance values of the near infrared, SWIR2, blue, and red bands.

After the development of spectral indices, 800 ground sample points, 200 for each land cover type are collected from the high-resolution images and visual image interpretation. The ground sample points are randomly selected from the entire study area to ensure potential variability in the surface reflectance. Then, the corresponding spectral values are extracted and plotted (Fig. 1). Third, spectral separability analysis is conducted, and the typical statistics of the spectral indices are computed. Fourth, considering the typical statistics of adjacent land covers, the optimized threshold (OT) is computed using (4) [10]. Fifth, optimized thresholds are imputed to classify land covers using a non-parametric decision tree (DT) algorithm (Fig. 2).

$$T_o = \left(\frac{X_{\mu'} + Y_{\mu''}}{2}\right) + \sigma \quad (4)$$

where T_0 is the optimized threshold between adjacent land covers, $X_{\mu'}$ & $Y_{\mu''}$ indicate the observed minimum and maximum mean values of adjacent land covers, and σ is the standard deviation of the mean of less than mean and mean of greater than mean, and mean reflectance (5).

$$T_\mu = \frac{1}{n}\sum_{i=1}^{n} X_i \quad (5)$$

where T_μ is the mean threshold, n is the total number of ground samples, and X_i is the spectral reflectance of *ith*

observed points for a particular land cover.

Finally, the accuracy assessment measures are computed for evaluating the performance of the spectral indices for multi-temporal urban land cover mapping. In this research, 2000 ground truth data are used, and the accuracy of results are estimated in terms of overall accuracy (OA), producer accuracy (PA), user accuracy (UA) and kappa coefficient (*k*).

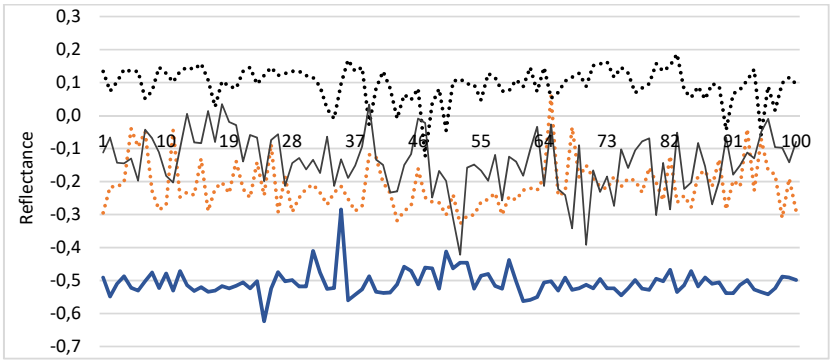

(a) Landsat-7 ETM

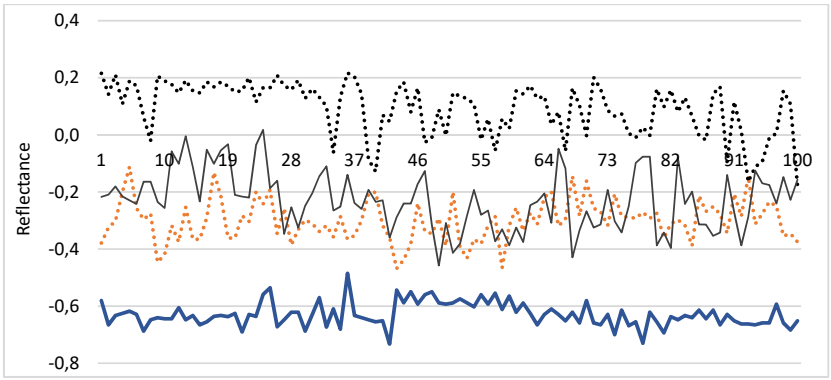

(b) Landsat-5 TM

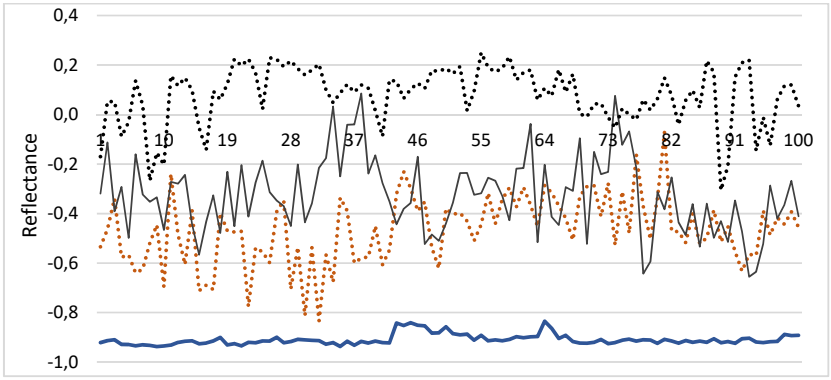

(c) Landsat-8 OLI

Fig. 1 MNDBI reflectance of the land cover classes. Legend: bare land (black dot), vegetation (orange dot), impervious (black) and water (dark blue). Note: the horizontal axis represents number of sample pixels

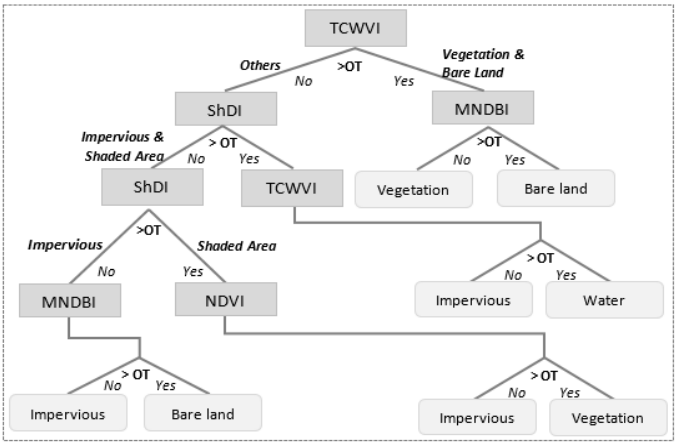

Fig. 2 Workflow for the proposed approach of land cover classification

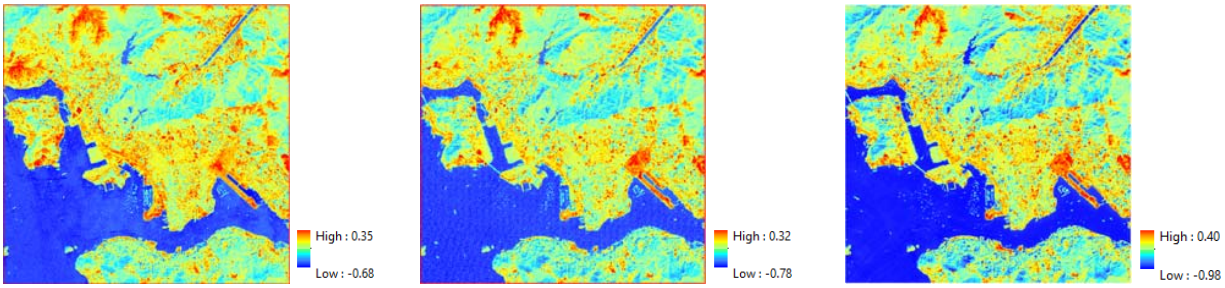

(a) Landsat-7 ETM (b) Landsat-5 TM (c) Landsat-8 OLI

Fig. 3 Multi-temporal MNDBI Maps

TABLE III
COMPARISON OF TYPICAL STATISTICS OF THE MNDBI FOR DIFFERENT LAND COVER CLASSES

Statistics	Landsat ETM				Landsat TM				Landsat OLI			
	SW	V	BL	IA	SW	V	BL	IA	SW	V	BL	IA
Max	-0.28	0.06	0.19	0.03	-0.49	-0.11	0.22	0.02	-0.83	-0.07	0.25	0.09
Min	-0.62	-0.33	-0.12	-0.42	-0.73	-0.47	-0.18	-0.46	-0.94	-0.83	-0.31	-0.66
Mean	-0.51	-0.21	0.10	-0.14	-0.63	-0.30	0.09	-0.23	-0.91	-0.47	0.08	-0.33
Stdv	0.04	0.07	0.05	0.09	0.04	0.07	0.09	0.10	0.02	0.14	0.12	0.15

III. EXPERIMENTAL EVALUATION AND RESULTS

First, this paper presents the results of the comparative analysis of the spectral indices delineated from multiple sensors. Second, this paper describes the performance evaluation results of the spectral indices for multi-temporal urban land cover mapping.

A. Comparison of Spectral Indices from Multiple Sensors

1. Evaluation of the MNDBI

Fig. 3 shows the delineated maps of the MNDBI for the three sensors of Hong Kong. The lowest values indicate water and the highest values indicate bare land. In contrast, the intermediate values indicate impervious and vegetation of both study areas. Table III presents the typical statistics of the MNDBI. The results indicate that the minimum, maximum, mean and standard deviations of the MNDBI are variable to sensors.

The investigations confirm although the typical statistics of the MNDBI are influenced by the spatial and temporal variations, this index yields the highest positive mean values for bare lands (Table III) for all data types thus facilitates its separation from impervious areas. Importantly it is noted that the variation in sensors influences the spectral reflectance thus careful consideration should be given to determine the threshold of MNDBI to separate bare land from impervious areas using multi-temporal data.

2. Evaluation of the TCWVI

Fig. 4 shows the delineated maps of the TCWVI for the three sensors of Hong Kong. The lowest values indicate vegetation and the highest values indicate water. In contrast, the intermediate values indicate impervious and bare lands of both study areas. Table IV presents the typical statistics of the TCWVI for the Hong Kong datasets. The results indicate that the minimum, maximum, mean and standard deviations of the

TCWVI are variable to sensors.

The investigations confirm although the typical statistics of the TCWVI are influenced by the spatial and temporal variations, this index yields the highest positive mean values for water and lowest mean values for vegetation (Table IV) for all the sensors thus the TCWVI can be used to detect these two land covers simultaneously. Importantly it is noted that the variation in sensors influence ground reflectance thus careful consideration should be given to choosing thresholds of TCWVI to separate these land covers using multi-temporal data.

3. Evaluation of the ShDI

The ShDI is delineated to maximize the spectral reflectance between building shadows and water. The skyscrapers of Hong Kong throw shadows that create problems in the analysis of low-resolution images thus the ShDI maps are delineated as shown in Fig. 5. The highest values indicate water and the lowest values indicate bare land and vegetation. In contrast, the intermediate values indicate shadows and impervious areas.

Table V presents the typical statistics of the ShDI for the Hong Kong datasets. The results indicate that the typical statistics of the ShDI are variable to sensors. However, the ShDI yields the highest positive mean values for water and maximizes spectral separability from shadow for all the sensors. Although, the ShDI enhances the separation between water and shadow. Its efficiency of separation is high for Landsat OLI data compared to Landsat ETM and TM data. Because the differences of mean reflectance of water, shadow, and impervious areas are significant for OLI data (Table V). In contrast, Landsat ETM and TM data to some extent separate shadows from water but show no significant spectral difference between impervious and shaded areas. The investigations confirm that the ShDI enhance water detection by separating shadows. However, the use of Landsat-OLI data results in the highest spectral separability compared to other sensors. As the performance of the ShDI is variable to sensors, thus careful consideration should be given to choosing the ShDI threshold values to separate shadows from water areas.

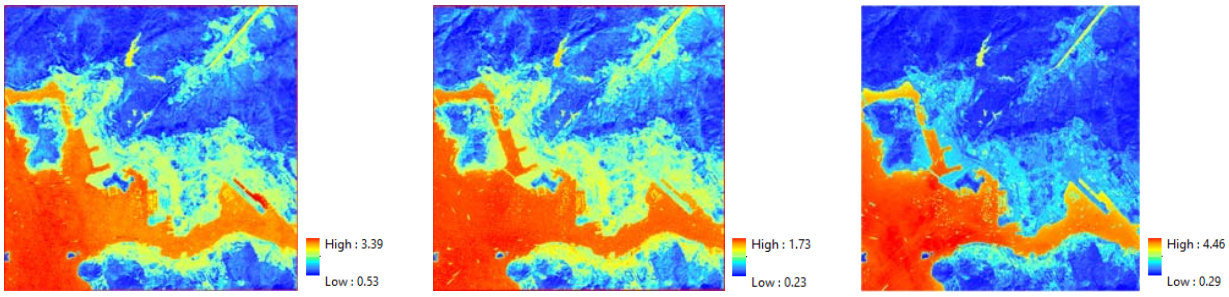

(a) Landsat-7 ETM (b) Landsat-5 TM (c) Landsat-8 OLI

Fig. 4 Multi-temporal TCWVI maps

TABLE IV
COMPARISON OF TYPICAL STATISTICS OF THE TCWVI FOR DIFFERENT LAND COVER CLASSES

Statistics	Landsat ETM				Landsat TM				Landsat OLI			
	SW	V	BL	IA	SW	V	BL	IA	SW	V	BL	IA
Max	3.12	1.14	1.32	1.97	1.60	0.66	0.71	1.21	4.06	1.24	1.00	2.15
Min	1.85	0.58	0.82	1.68	1.14	0.25	0.37	0.86	2.36	0.38	0.65	1.14
Mean	2.45	0.76	1.04	1.80	1.42	0.41	0.59	1.03	3.26	0.59	0.77	1.60
Stdv	0.24	0.09	0.08	0.07	0.12	0.08	0.05	0.06	0.46	0.15	0.08	0.20

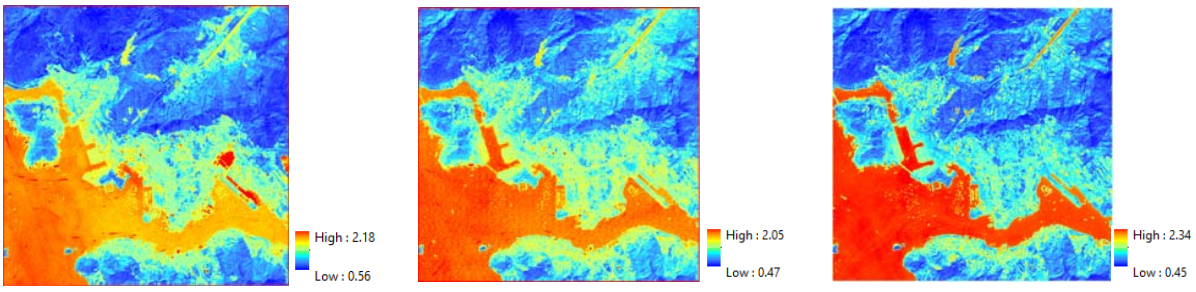

(a) Landsat-7 ETM (b) Landsat-5 TM (c) Landsat-8 OLI

Fig. 5 Multi-temporal ShDI maps

TABLE V
COMPARISON OF TYPICAL STATISTICS OF THE SHDI FOR DIFFERENT LAND COVER CLASSES AND SHADOW (Sd)

Statistics	Landsat ETM					Landsat TM					Landsat OLI				
	SW	V	BL	IA	Sd	SW	V	BL	IA	Sd	SW	V	BL	IA	Sd
Max	1.52	0.86	0.80	1.26	1.18	1.48	0.92	0.78	1.38	1.27	1.75	1.21	0.81	1.39	1.59
Min	1.03	0.60	0.63	0.79	0.93	1.15	0.63	0.57	0.92	0.95	1.51	0.57	0.53	0.89	1.07
Mean	1.23	0.70	0.68	1.01	1.05	1.33	0.76	0.66	1.06	1.12	1.62	0.76	0.62	1.07	1.36
Stdv	0.08	0.05	0.03	0.08	0.05	0.07	0.06	0.05	0.07	0.06	0.06	0.12	0.07	0.09	0.11

TABLE VI
ACCURACY OF RESULTS (%) FOR MULTIPLE SENSOR DATASET

Land Covers	Landsat-7 ETM				Landsat-5 TM				Landsat-8 OLI			
	PA	UA	OA	*k*	PA	UA	OA	*k*	PA	UA	OA	*k*
Water	98.2	96.3			95.8	95.6			99.4	99.9		
Vegetation	99.7	94.2			99.5	88.8			98.7	94.9		
Impervious	97.3	98.6			88.9	96.1			94.5	97.8		
Bare land	81.0	98.7			84.0	93.3			86.0	87.9		
			96.6	0.95			93.3	0.91			96.1	0.95

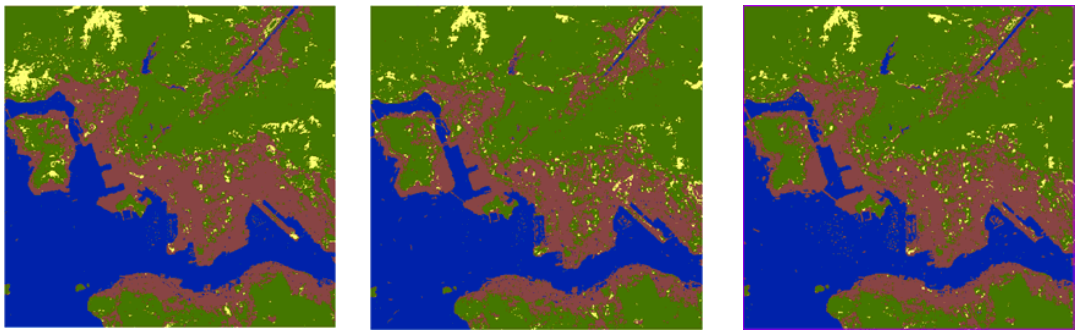

(a) Landsat-7 ETM (a) Landsat-5 TM (c) Landsat-8 OLI

Fig. 6 Multi-temporal land cover maps derived from spectral indices. Legend: bare land (light yellow), vegetation (green), impervious (brown) and water (blue)

B. Multi-Temporal Land Cover Mapping Based on Spectral Indices

This section presents the results of multi-temporal land cover maps of Hong Kong. The land cover maps are derived using the optimized thresholds of the spectral indices. A non-parametric DT algorithm is implemented based on optimized thresholds of the spectral indices. Fig. 6 presents the results of multi-temporal land cover maps and Table VI shows the accuracy of the results of the proposed approach of land cover classification. The assessment indicates that the spectral indices based classification approach is most accurate to classify water followed by vegetation. In contrast, the least accuracy is observed for bare land; however, the proposed approach improves its separation from impervious area. The results indicate the classification accuracy is variable to sensors. The highest accuracy is observed for Landsat ETM and OLI data and lowest for Landsat TM data. Overall, the approach has an accuracy of 93-96% for the Hong Kong datasets. In conclusion, the investigations confirm that the development of MNDBI, TCWVI and ShDI using multiple sensors is competent to map multi-temporal urban land covers. The results of the assessment are consistent with those findings of Faridatul and Wu [10].

IV. CONCLUSIONS AND DISCUSSION

This paper presents the performance of the three spectral indices to enhance urban land cover mapping using multi-sensor Landsat data. The results indicate that the MNDBI, TCWVI and ShDI spectral indices characterize similar pattern in the distribution of land covers but the typical statistics of the spectral indices are variable to sensors. Various factors e.g., atmospheric transmission, cloud, wind, image acquisition time, vegetation types and the characteristics of the physical properties altogether can affect the spectral reflectance. Thus, careful consideration should be given to choosing spectral thresholds to detect land cover types for different sensors and urban areas. This research develops a ShDI, however, the index is important to consider in urban areas where skyscrapers throw shadow.

The experimental results and comparison analysis confirm that the MNDBI provides the highest spectral reflectance for bare land and maximize spectral separability from impervious areas. The TCWVI yields the highest spectral reflectance for water and lowest for vegetation, which facilitates simultaneous detection of water and vegetation. The ShDI index maximizes the reflectance between water and shadow thus improves water detection. However, the performance of the ShDI is

robust to Landsat OLI data compared to other sensors. The experimental evaluation demonstrates that the spectral indices facilitate a reliable multi-temporal land cover mapping using Landsat ETM, TM and OLI data that provides between 93-96% accuracy. The overall results indicate that the proposed spectral indices are of significance to map multi-temporal urban land covers for monitoring urban sprawl and managing the ecology.

ACKNOWLEDGMENT

The work was supported by the Hong Kong PhD Fellowship. The authors thank the Research Grant Council of Hong Kong for providing funding and thank the US Geological Survey (USGS) for making the Landsat datasets publicly available.

REFERENCES

[1] I. Doustfatemeh and Y. Baleghi, "Comprehensive urban area extraction from multispectral medium spatial resolution remote-sensing imagery based on a novel structural feature," *International Journal of Remote Sensing,* vol. 37, pp. 4225-4242, 2016.

[2] W. D. Shuster, J. Bonta, H. Thurston, E. Warnemuende, and D. R. Smith, "Impacts of impervious surface on watershed hydrology: A review," *Urban Water Journal,* vol. 2, pp. 263-275, 2005.

[3] E. Li, P. Du, A. Samat, J. Xia, and M. Che, "An automatic approach for urban land-cover classification from Landsat-8 OLI data," *International Journal of Remote Sensing,* vol. 36, pp. 5983-6007, 2015.

[4] J. Dujardin, O. Batelaan, F. Canters, S. Boel, C. Anibas, and J. Bronders, "Improving surface–subsurface water budgeting using high resolution satellite imagery applied on a brownfield," *Science of the Total Environment,* vol. 409, pp. 800-809, 2011.

[5] J. Paneque-Gálvez, J.-F. Mas, G. Moré, J. Cristóbal, M. Orta-Martínez, A. C. Luz, *et al.*, "Enhanced land use/cover classification of heterogeneous tropical landscapes using support vector machines and textural homogeneity," *International Journal of Applied Earth Observations and Geoinformation,* vol. 23, pp. 372-383, 2013.

[6] X. Chen, J. Chen, Y. Shi, and Y. Yamaguchi, "An automated approach for updating land cover maps based on integrated change detection and classification methods," *ISPRS Journal of Photogrammetry and Remote Sensing,* vol. 71, pp. 86-95, 2012/07/01 2012.

[7] C. He, P. Shi, D. Xie, and Y. Zhao, "Improving the normalized difference built-up index to map urban built-up areas using a semiautomatic segmentation approach," *Remote Sensing Letters,* vol. 1, pp. 213-221, 2010.

[8] X. Li, X. Liu, and L. Yu, "Aggregative model-based classifier ensemble for improving land-use/cover classification of Landsat TM Images," *International Journal of Remote Sensing,* vol. 35, pp. 1481-1495, 2014.

[9] G. Li and Y. Wan, "A new combination classification of pixel- and object-based methods," *International Journal of Remote Sensing,* vol. 36, pp. 5842-5868, 2015.

[10] M. I. Faridatul and B. Wu, "Automatic classification of major urban land covers based on novel spectral indices," *ISPRS International Journal of Geo-Information,* vol. 7, pp. 1-24, 2018.

[11] A. Hamedianfar, H. Z. M. Shafri, S. Mansor, and N. Ahmad, "Improving detailed rule-based feature extraction of urban areas from WorldView-2 image and lidar data," *International Journal of Remote Sensing,* vol. 35, pp. 1876-1899, 2014.

[12] Y. Zha, J. Gao, and S. Ni, "Use of normalized difference built-up index in automatically mapping urban areas from TM imagery," *International Journal of Remote Sensing,* vol. 24, pp. 583-594, 2003.

[13] S. K. McFeeters, "The use of the normalized difference water index (NDWI) in the delineation of open water features," *International Journal of Remote Sensing,* vol. 17, pp. 1425-1432, 1996.

[14] H. Xu, "A study on information extraction of water body with the modified normalized difference water index (MNDWI)," *Journal of Remote Sensing,* vol. 9, pp. 589-595, 2005.

[15] J. W. Rouse, R. H. Haas, J. A. Schell, and D. W. Deering, "Monitoring vegetation systems in the great plains with ERTS," in *Third 80 ERTS Symposium*, 1973, pp. 309-317.

[16] R. Amine and F. Hadria, "Integration of NDVI indices from the tasseled cap transformation for change detection in satellite images," *International Journal of Computer Science Issues (IJCSI),* vol. 9, pp. 172-177, 2012.

[17] A. Bhatt, S. K. Ghosh, and A. Kumar, "Spectral indices based object oriented classification for change detection using satellite data," *International Journal of System Assurance Engineering and Management,* vol. 9, 33-42, 2016.

[18] M. K. Ridd, "Exploring a V-I-S (vegetation-impervious surface-soil) model for urban ecosystem analysis through remote sensing: comparative anatomy for cities†," *International Journal of Remote Sensing,* vol. 16, pp. 2165-2185, 1995/08/01 1995.